Available online at www.sciencedirect.com
SCIENCE DIRECT®
Journal of Power Sources 119–121 (2003) 626–630
JOURNAL OF POWER SOURCES
www.elsevier.com/locate/jpowsour

Phase transition in the spinel $Li_4Ti_5O_{12}$ induced by lithium insertion Influence of the substitutions Ti/V, Ti/Mn, Ti/Fe

Pierre Kubiak, Aurélie Garcia, Manfred Womes, Laurent Aldon, Josette Olivier-Fourcade, Pierre-Emmanuel Lippens, Jean-Claude Jumas*

Laboratoire des Agrégats Moléculaires et Matériaux Inorganiques (UMR 5072 CNRS), Université Montpellier II, CC15, Place Eugène Bataillon, 34095 Montpellier Cedex 5, France

Abstract

The spinel $Li_4Ti_5O_{12}$, a stable phase of the Li_2O–TiO_2 system, allows to insert three Li atoms per formula unit at a potential of 1.5 V on the basis of a spinel ↔ NaCl phase transition. This mechanism leads to a reduction of three Ti(IV) atoms out of five, corresponding to a theoretical capacity of 175 mAh/g. The influence of structural defaults on the spinel → NaCl phase transition and its reversibility during charge/discharge cycles have been studied. Solid solutions formed from chemical insertion of lithium or substitutions Ti/V, Ti/Mn, Ti/Fe modify the cation distribution on the crystallographic sites (tetrahedral 8a, octahedral 16d, space group *Fd3m*) and influence the electrochemical performances. A structural analysis by X-ray and neutron diffraction, X-ray absorption, ^{57}Fe Mössbauer spectroscopy and first principle calculations have allowed to establish a relationship between the structure and the electrochemical properties.

Keywords: $Li_4Ti_5O_{12}$; Anode; Li-ion batteries; Insertion mechanisms; ^{57}Fe Mössbauer data

1. Introduction

The development of high energy and power batteries is expected to ensure new applications in the field of portable power tools and hybrid vehicles. Commercially available lithium batteries use carbon or graphite as the anode material. Their electrochemical potential lies close to 0 V versus lithium, which causes serious safety problems. In order to solve the limitations of present Li-ion battery technology, it could be interesting to shift the voltage window of the battery from the usual 0–4 V of lithium-ion to 1–5 V range. It is therefore important to find new anode materials working at higher potentials (around 1 V) [1]. Titanium oxides fulfil this requirement. The spinel $Li_4Ti_5O_{12}$ (partial inverted spinel (Li) $[Li_{0.33}Ti_{1.67}]O_4$), a stable phase of the Li_2O–TiO_2 system, allows to insert three Li atoms per formula unit at a potential of 1.5 V [2–8] according to an insertion mechanism on the basis of a spinel ↔ NaCl phase transition [9,10]. This mechanism leads to a reduction of three Ti(IV) atoms out of five, corresponding to a theoretical capacity of 175 mAh/g. Tests showed the mechanism to be of high reversibility [5,6].

In the present paper, we investigate the influence of structural defaults induced by lithium insertion or substitutions Ti/V, Ti/Mn, and Ti/Fe in a solid solution range on the spinel → NaCl phase transition and its reversibility during charge/discharge cycles. A structural analysis by X-ray and neutron diffraction, ^{57}Fe Mössbauer spectroscopy of the Fe-substituted phase and first principle calculations have allowed us to establish a relationship between structure and electrochemical properties.

2. Experimental and theoretical methods

The spinel phase $Li_4Ti_5O_{12}$ is obtained by sol–gel as well as ceramic synthesis routes, using various precursors (Li_2CO_3, LiOH, TiO_2, $Ti(OiPr)_4$, $Li(CH_3CO_2)\cdot 2H_2O$). Substituted spinels have been precipitated from solutions of titanium iso-propoxide and various lithium and dopant precursors ($FeCl_3\cdot 6H_2O$, $MnCl_4\cdot 4H_2O$ and V(acac)). Iron doping was alternatively carried out from iron metal powder enriched in the isotope ^{57}Fe in order to introduce a probe for ^{57}Fe Mössbauer spectroscopy. The chemical insertion of lithium has been carried out using *n*-butyl lithium.

* Corresponding author.
E-mail address: jumas@univ-montp2.fr (J.-C. Jumas).

0378-7753/03/$ – see front matter
doi:10.1016/S0378-7753(03)00186-1

Electrochemical lithiation was carried out with (Li/$LiPF_6$ 1 M (EC:DMC)/lithium titanate) Swagelock™ test cells as described in [11]. Galvanostatic discharge/charge curves were obtained with a cycling rate of 1 Li/5 h. Electrochemically inserted samples for Mössbauer characterisation were prepared using a slow rate of 1 Li/20 h.

Pristine and lithiated samples were characterised by X-ray powder diffraction (XPD) with a Philips θ–2θ diffractometer using Cu Kα radiation and a nickel filter. The chemically inserted lithium sample has been studied by neutron powder diffraction (NPD) on D1B at ILL (Grenoble, France). Rietveld refinements were carried out with the program DBWS-9411 [12].

The iron doped spinel and some samples at several depths of discharge and charge have been characterised by ^{57}Fe Mössbauer spectroscopy at room temperature with a classical EG & G constant accelerator spectrometer in transmission mode using a ^{57}Co in a Rh matrix as γ-ray source. The velocity scale was calibrated using the magnetic sextuplet spectrum of a high purity iron foil absorber and the origin of the isomer shift scale was determined from the centre of the α-Fe spectrum. For the electrochemically inserted samples the measurements were performed ex situ from Swagelock electrodes. Experimental data were analysed by evaluation of hyperfine parameter distributions [13].

The X-ray absorption spectroscopy (XAS) measurements were carried out at LURE (Orsay, France). The O K-edge spectra were recorded at Super ACO storage ring in the total electron yield mode using the SA72 beam line monochromator with an energy resolution of 0.2 eV. The samples were finely ground and dispersed in acetone and spread on a Ta sample holder and dried. The spectra were recorded in the range 510–575 eV.

The electronic structure of $Li_4Ti_5O_{12}$ has been evaluated from first principle calculations based on the density functional theory (DFT) within the generalised gradient approximation (GGA). The linearized augmented plane wave (LAPW) method has been used (WIEN code [14]). The XAS spectra have been calculated within the dipole approximation and core hole effects have been included by removing one O 1s electron. For a comparison with experiments, the calculated spectra have been broadened by a Lorentzian function with a full width at half maximum (FWHM) equal to 1 eV in order to take into account the finite lifetimes of both the core hole and the excited states, and the experimental resolution. Comparison between theoretical and experimental spectra allows to analyse the main peaks: the atomic contributions are determined by considering the calculated partial densities of states (DOS).

3. The $Li_4Ti_5O_{12}$ spinel compound

$Li_4Ti_5O_{12}$ has a cubic spinel structure (space group *Fd*3*m*) and the lattice constant is 8.368 (3) Å. The cationic repartition within the conventional cell of 56 atoms can be described by the formula

$$(Li_8)_{8a}\,[Li_{2.667}Ti_{13.333}]_{16d}\,O_{32}$$

where the subscripts 8a and 16d denote the tetrahedral (parentheses) and octahedral (brackets) crystallographic sites, respectively. The spinel–NaCl phase transition due to Li insertion is related to the change in the local Li site symmetry from (8a) to (16c) and to the occupation of the unoccupied (16c) sites by eight inserted lithium. The rock-salt compound can be described by

$$[Li_{16}]_{16c}\,[Li_{2.667}Ti_{13.333}]_{16d}\,O_{32}$$

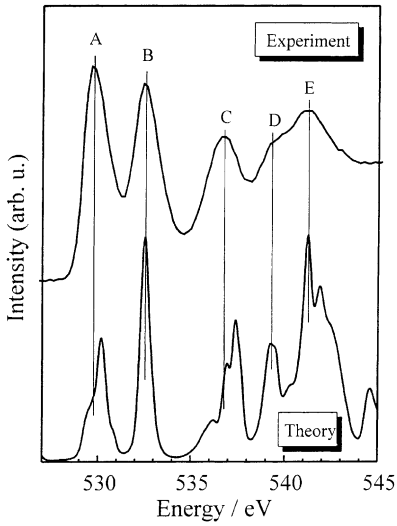

Fig. 1. Comparison between calculated and experimental XAS spectra of $Li_4Ti_5O_{12}$ at the O K edge.

The phase transition is related to the reduction of three titanium atoms from Ti(IV) to Ti(III). The change in the lithium site symmetry is of great importance for the insertion mechanisms and could be, in principle, followed by XAS at the O K edge as predicted from LAPW calculations. Calculated and experimental spectra of $Li_4Ti_5O_{12}$ in the energy range between 525 and 545 eV show the same main peaks labelled A–E (Fig. 1). The observed differences in the amplitudes of the peaks are mainly due to the energy dependent broadening caused by the finite lifetime of the excited states which is not considered in the present calculation. The analysis of the partial DOS allows to determine the character of these peaks in terms of orbital interactions. It can be shown that the empty states which contribute to the peak C are mainly due to the hybridisation between Li (8a) p-type orbitals and O 2p orbitals. There is no significant contribution of the Li atoms in octahedral sites. Thus, the peak C is expected to be modified by changes in Li site symmetry due to Li insertion.

4. The doped materials

The addition and substitution of atoms are expected to modify the crystal structure, the texture and the properties of

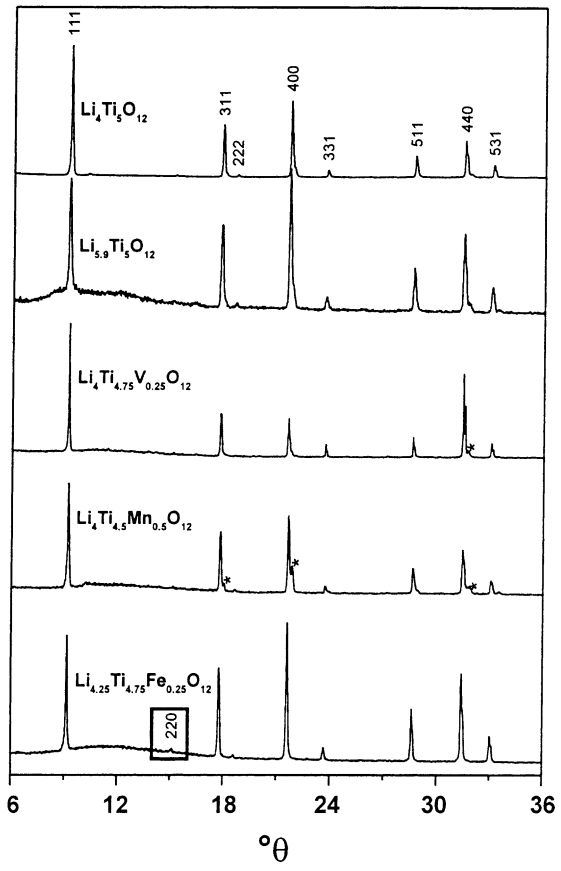

Fig. 2. XPD of $Li_4Ti_5O_{12}$ [$a = 8.368$ (3) Å], $Li_{5.9}Ti_5O_{12}$ [$a = 8.373$ (1) Å], $Li_4Ti_{4.75}V_{0.25}O_{12}$ [$a = 8.358$ (3) Å], $Li_4Ti_{4.5}Mn_{0.5}O_{12}$ [$a = 8.356$ (3) Å] and $Li_{4.25}Ti_{4.75}Fe_{0.25}O_{12}$ [$a = 8.359$ (2) Å]; (∗) impurity of Li_2TiO_3.

Table 1
^{57}Fe Mössbauer data of $Li_4Ti_{4.75}Fe_{0.25}O_{11.88}$ and corresponding discharged electrodes at 1.9, 1.6, 1.5 and 1 V

Sample	δ (mm/s)	Δ (mm/s)	Γ (mm/s)	Contribution (%)
$Li_4Ti_{4.75}Fe_{0.25}O_{12}$	0.22 (1)	0.29 (1)	0.35 (1)	32.8
	0.32 (1)	0.65 (1)	0.66 (1)	67.2
Discharge	0.29 (1)	0.26 (1)	0.40 (3)	26.0
1.9 V	0.35 (1)	0.67 (1)	0.29 (2)	12.7
0.149 Li	0.92 (1)	1.16 (1)	0.85 (2)	61.3
Discharge	0.20 (1)	0.18 (1)	0.29 (2)	17.6
1.6 V	1.00 (1)	0.66 (1)	0.41 (2)	30.4
0.251 Li	1.03 (1)	1.14 (1)	0.41 (2)	30.5
	0.97 (1)	1.94 (2)	0.41 (2)	21.5
Discharge	1.01 (1)	0.55 (1)	0.41 (3)	23.1
1.5 V	1.01 (1)	1.00 (1)	0.41 (3)	31.1
2.032 Li	1.01 (1)	1.45 (2)	0.41 (3)	24.0
	1.01 (1)	1.94 (1)	0.41 (3)	21.8
Discharge	1.03 (1)	0.50 (1)	0.43 (2)	18.9
1.0 V	1.01 (1)	0.94 (1)	0.43 (2)	31.0
2.196 Li	1.01 (1)	1.40 (1)	0.43 (2)	28.9
	1.01 (1)	1.91 (1)	0.43 (2)	21.2

δ, isomer shift relative to α Fe; Δ, quadrupole splitting; Γ, line width.

the materials, and therefore to change the electrochemical performances of $Li_4Ti_5O_{12}$. The composition $Li_{5.9}Ti_5O_{12}$ has been obtained by chemical insertion of lithium with *n*-butyl lithium. The substitution of Ti atoms by V, Fe (5%) and Mn (10%) has been realised by mixed sol–gel ceramic routes.

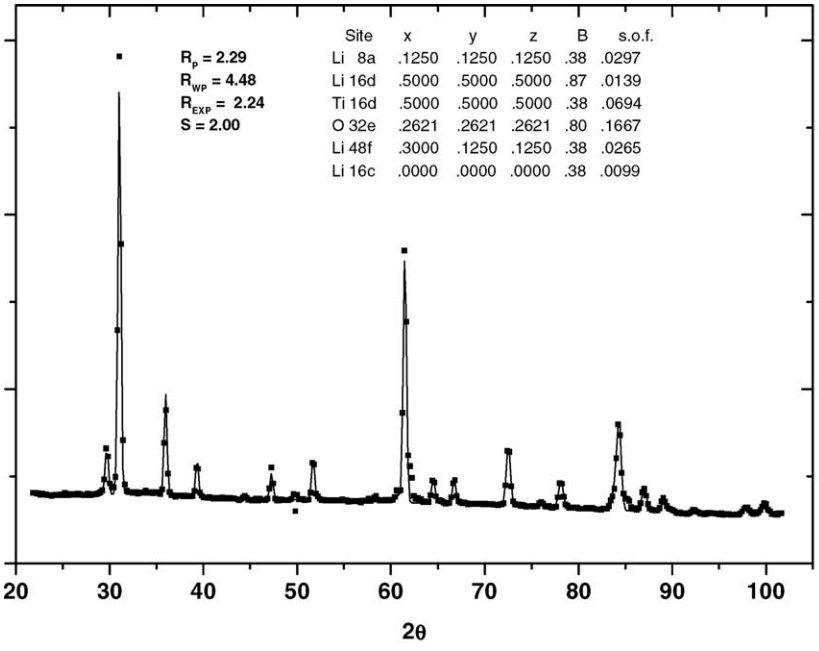

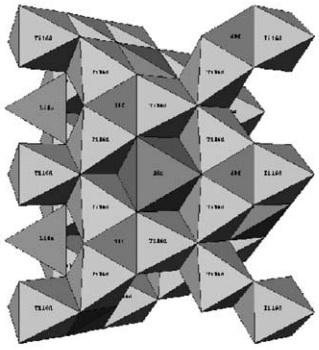

$$(Li_{5.7}\square_{2.3})_{8a}\,[Li_{8/3}Ti_{40/3}]_{16d}\{Li_{5,1}\square_{42.9}\}_{48f}\,[Li_{1.9}\square_{14.1}]_{16c}O_{32}$$

Fig. 3. Rietveld analysis of NPD for $Li_{5.9}Ti_5O_{12}$ showing lithium insertion on interstitial sites 48f and 16c (space group *Fd3m*).

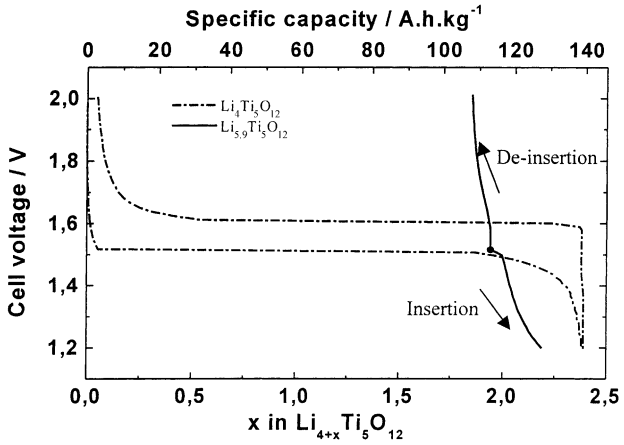

Fig. 4. Typical charge and discharge curves of chemically inserted spinel $Li_{5.9}Ti_5O_{12}$ and comparison with $Li_4Ti_5O_{12}$.

For $Li_{5.9}Ti_5O_{12}$, the XPD patterns (Fig. 2) do not show significant differences. The analysis of the NPD pattern obtained for the spinel phase after chemical Li insertion shows that lithium are inserted not only in octahedral (16c) but also in tetrahedral (48f) sites of the spinel lattice (Fig. 3). Fig. 4 shows very poor electrochemical performances for the chemically inserted material due to the occupation of the 48f tetrahedral sites which prevents the phase transition.

The spinels with 5% of Ti substituted by V ($Li_4Ti_{4.75}V_{0.25}O_{12}$) or Fe ($Li_4Ti_{4.75}Fe_{0.25}O_{11.88}$), or 10% by Mn ($Li_4Ti_{4.50}Mn_{0.50}O_{12}$) have been examined by XPD (Fig. 2). Fe and V doped spinels were obtained in pure form, Mn doped spinel contain impurities of Li_2TiO_3. In order to optimise the conditions favouring the spinel ↔ rocksalt transition, it is of interest to analyse the loss of capacity (Fig. 5) induced from the substitutions and to understand the observed changes as a function of the dopant.

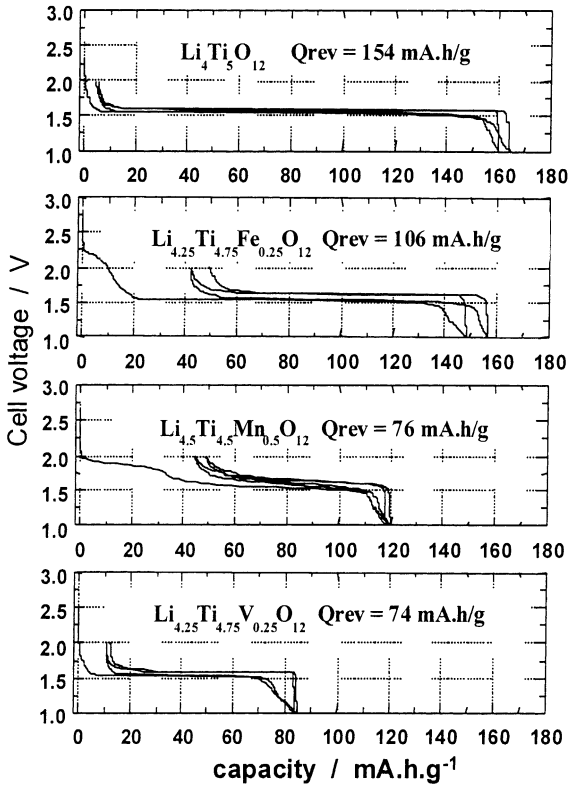

Fig. 5. Typical charge and discharge curves of spinel $Li_4Ti_5O_{12}$ and substituted compounds with Fe, Mn and V.

The substitutions Ti/V, Ti/Mn, and Ti/Fe modify the cation distribution on the sites in agreement with previous results [15–17]. ^{57}Fe Mössbauer spectroscopy shows that Fe dopants have been introduced in the spinel lattice as Fe(III) on both octahedral (16d) and tetrahedral (8a) sites (Fig. 6 and Table 1). The latter result is confirmed by XPD with the appearance of the (2 2 0) diffraction peak at $\theta = 15.10°$

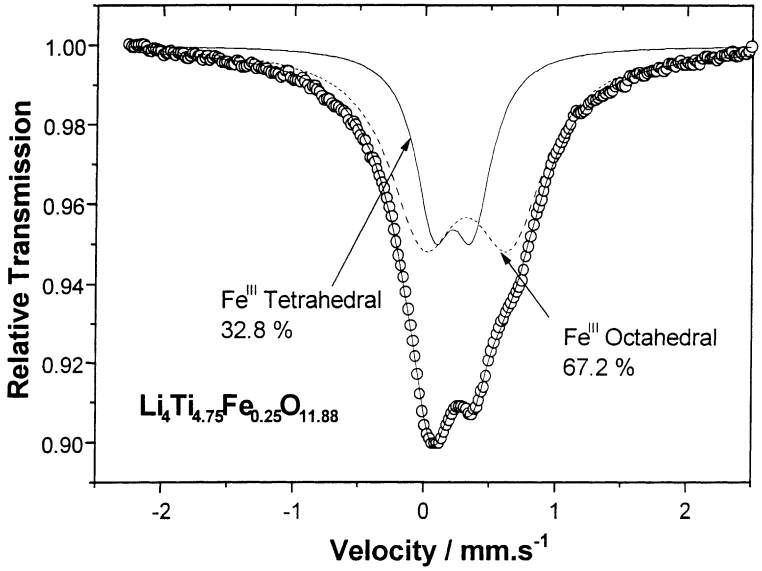

Fig. 6. ^{57}Fe Mössbauer spectrum of $Li_4Ti_{4.75}Fe_{0.25}O_{11.88}$: experimental and calculated data.

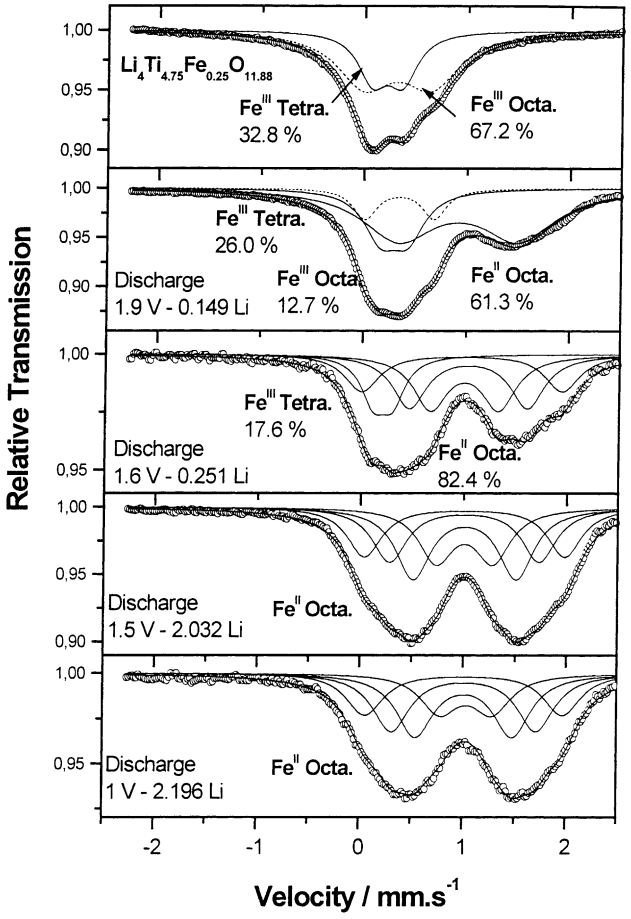

Fig. 7. Experimental and fitted ^{57}Fe Mössbauer spectra for $Li_4Ti_{4.75}Fe_{0.25}O_{11.88}$ and corresponding discharged electrodes at 1.9, 1.6, 1.5 and 1 V.

which is characteristic of the occupation of the tetrahedral sites by heavier elements than Li (Fig. 2). During the first discharge the Fe(III) ions are reduced into Fe(II) (Fig. 7 and Table 1), which can be explained by the migration of the Fe atoms from tetrahedral to octahedral sites. The discharge is complete at 1 V and all the Fe sites are octahedral. This mechanism corresponds to the spinel–NaCl phase transition.

XAS at the V L(III) absorption edge lets conclude that V is mainly entered as V(IV) on octahedral sites. Measurements at the Mn K-edge show that Mn is located as Mn(IV) probably on both octahedral and tetrahedral sites. As for iron doped compounds, these results can be related to the observed irreversible insertion mechanisms during the first discharge (Fig. 5).

5. Conclusion

The electrochemical insertion mechanism in $Li_4Ti_5O_{12}$ is based on the reversible spinel–NaCl phase transformation

$$Li_4Ti_5O_{12} + 3Li \leftrightarrow Li_7Ti_5O_{12}$$

The theoretical capacity is 175 mAh/g. We have shown that the electrochemical performances are strongly related to the existence of defects in the material: the octahedral defects (16d) reduce the capacity and the tetrahedral defects (8a) create an irreversible insertion mechanism.

The substitutions Ti/V, Ti/Mn, and Ti/Fe modify the cation distribution on the sites (tetrahedral 8a, octahedral 16d), change the texture and influence the electrochemical performances by decreasing the mass capacities. Introduction of lithium on interstitial sites 48f by chemical insertion prevents the phase transition.

Acknowledgements

The authors would like to thank C. Siret, Ph. Biensan (SAFT), A. Audemer, J. Scoyer (UMICORE) for fruitful discussions and electron microscopy studies and the EC for funding (NEGELiA contract ENK6-CT-2000-00082).

References

[1] E. Ferg, R.J. Gummov, A. de Kock, M.M. Thackeray, J. Electrochem. Soc. 141 (1994) 147.
[2] T. Ohzuku, A. Ueda, N. Yamamoto, J. Electrochem. Soc. 142 (1995) 1431.
[3] S. Sarciaux, A. Le Gal La Salle, D. Guyomard, Y. Piffard, Mol. Cryst. Liq. Cryst. 311 (1998) 63.
[4] S.I. Pyun, S.W. Kim, H.C. Shin, J. Power Sources 81–82 (1999) 248.
[5] K. Zaghib, M. Simoneau, M. Armand, M. Gauthier, J. Power Sources 81–82 (1999) 300.
[6] A.N. Jansen, A.J. Kahaian, K.D. Kepler, P.A. Nelson, K. Amine, D.W. Dees, D.R. Vissers, M.M. Thackeray, J. Power Sources 81–82 (1999) 902.
[7] S. Bach, J.P. Pereira-Ramos, N. Baffier, J. Power Sources 81–82 (1999) 273.
[8] P.P. Prosini, R. Mancini, L. Petrucci, V. Contini, P. Villano, Solid State Ionics 144 (2001) 185.
[9] S. Scharner, W. Weppner, P. Schmid-Beurmann, J. Electrochem. Soc. 146 (1999) 857.
[10] S. Panero, P. Reale, F. Ronci, V. Rossi Albertini, B. Scrosati, Ionics 6 (2000) 461.
[11] S. Denis, E. Baudrin, M. Touboul, J.M. Tarascon, J. Electrochem. Soc. 144 (1997) 4099.
[12] R. Young, A. Sakthivel, T.S. Moss, C.O. Paiva-Santos, J. Appl. Crystallogr. 28 (1995) 366.
[13] G. Le Caer, J.M. Dubois, J. Phys. E: Sci. Instrum. 12 (1979) 1083.
[14] P. Blaha, K. Schwarz, J. Luitz, Proceedings of the Wien 97, Vienna University of Technology, Vienna, 1997 (updated version), Phys. Rev. Lett. 54 (1985) 1192.
[15] A.D. Roberston, H. Tukamoto, J.T.S. Irvine, J. Electrochem. Soc. 146 (1999) 3958.
[16] A.D. Roberston, L. Trevino, H. Yukamoto, J.T.S. Irvine, J. Power Sources 81–82 (1999) 352.
[17] S. Scharner, W. Weppner, P. Schmid-Beurmann, J. Solid State Chem. 134 (1997) 170.